A Ralstonia solanacearum phage RP15 is closely related to Viunalikeviruses and encodes 19 tRNA-related sequences

AUTHOR(S):

Mihara, Tomoko; Nasr-Eldin, Mohamed A.; Chatchawankanphanich, Orawan; Bhunchoth, Anjana; Phironrit, Namthip; Kawasaki, Takeru; Nakano, Miyako; Fujie, Makoto; Ogata, Hiroyuki; Yamada, Takashi

CITATION:

Mihara, Tomoko ...[et al]. A Ralstonia solanacearum phage RP15 is closely related to Viunalikeviruses and encodes 19 tRNA-related sequences. Virology Reports 2016, 6: 61-73

ISSUE DATE:

2016-12

URL:

http://hdl.handle.net/2433/218926

Virology Reports 6 (2016) 61–73

Contents lists available at ScienceDirect

Virology Reports

journal homepage: www.elsevier.com/locate/virep

A *Ralstonia solanacearum* phage ϕRP15 is closely related to *Viunalikeviruses* and encodes 19 tRNA-related sequences

Tomoko Mihara [a,1], Mohamed A. Nasr-Eldin [b,1], Orawan Chatchawankanphanich [c], Anjana Bhunchoth [c], Namthip Phironrit [c], Takeru Kawasaki [d], Miyako Nakano [d], Makoto Fujie [d], Hiroyuki Ogata [a,*], Takashi Yamada [d,**]

[a] *Bioinformatics Center, Institute for Chemical Research, Kyoto University, Uji, Kyoto 611-0011, Japan*
[b] *Department of Botany, Faculty of Science, Benha University, Qalubiya Governorate, 13511, Egypt*
[c] *Plant Research Laboratory, National Center for Genetic Engineering and Biotechnology, NSTDA, Pathum Thani 12120, Thailand*
[d] *Department of Molecular Biotechnology, Graduate School of Advanced Sciences of Matter, Hiroshima University, Higashi-Hiroshima 739-8530, Japan*

ARTICLE INFO

Article history:
Received 1 July 2016
Received in revised form 22 July 2016
Accepted 22 July 2016
Available online 25 July 2016

Keywords:
Ralstonia solanacearum
T4-related phages
Viunalikevirus
tRNA-gene cluster

ABSTRACT

A T4-related phage infecting *Ralstonia solanacearum* was isolated in Thailand (ϕRP15). ϕRP15 virions showed unique morphology with star-like protrusions attached to the base plate via a stalk. The 168 kb genome sequence of ϕRP15 was determined and found to encode 17 tRNAs (plus two tRNA pseudogenes). Ten of these phage-encoded tRNAs corresponded to codons that are relatively abundant in the phage but rare in the host, while others matched to codons frequent in both phage and host. Phylogenetic and proteomic analyses demonstrate that ϕRP15 forms a clade with *Delftia* phage ϕW-14, which in turn is placed as a sister group of viunalikeviruses. The hosts of ϕRP15 and ϕW-14 (*R. solanacearum* and *Delftia acidovorans*, respectively) belong to Betaproteobacteria, while most of the hosts of viunalikeviruses are of the *Enterobacteriaceae* belonging to Gammaproteobacteria. These phages may have evolved closely associated with their hosts that have very different life-styles in the natural habitats.

1. Introduction

T4-like phages classically representing *Myoviridae* phages have a contractile tail sheath and infect a broad range of bacterial hosts. Studies of T4-like phage genomes as models have suggested that myovirus genomes are mosaic of conserved core genes, which include structural genes for head and tail proteins and enzyme genes for DNA and nucleotide metabolism, and the remaining variable accessory non-core genes (Filee et al., 2006). The functions of non-core genes are largely unknown, although it is assumed that they provide a selective benefit to phages (Hendrix, 2009). Petrov and coworkers recently defined "T4-related phages" to group phages that share a "Core Genome" encoding approximately 37 proteins (Lavigne et al., 2009; Petrov et al., 2010). T4-related phages include the members of the genus *T4likevirus*, the genus *SchizoT4likevirus* (http://ictvonline.org) and other phages including cyanomyoviruses and *Delftia acidovorans* phage ϕW-14. More recently, another genus "*Viunalikevirus*" inside the T4-

* Corresponding author.
** Correspondence to: T. Yamada, Department of Molecular Biotechnology, Graduate School of Advanced Sciences of Matter, Hiroshima University, 1-3-1 Kagamiyama, Higashi-Hiroshima 739-8530, Japan.
E-mail addresses: ogata@kuicr.kyoto-u.ac.jp (H. Ogata), tayamad@hiroshima-u.ac.jp (T. Yamada).
[1] These authors contributed equally.

http://dx.doi.org/10.1016/j.virep.2016.07.001

related phages was proposed for phages showing a number of features that distinguish them from other members of the T4-related phages (Adriaenssens et al., 2012a). Viunalikeviruses are characterized as virulent phages showing similar genome size (150–170 kbp), extensive DNA homology, strong gene synteny, and a complex adsorption apparatus on the virion. Members of this genus include phages infecting bacterial hosts belonging to *Enterobacteriaceae* (Gammaproteobacteria).

The phytopathogen *Ralstonia solanacearum*, a soil-borne Gram-negative bacterium (Betaproteobacterium), causes bacterial wilt disease in many important crops (Hayward, 1991; Yabuuchi et al., 1995). The unusually wide host-range of this bacterium extends to over 200 species belonging to >50 botanical families (Hayward, 2000). *R. solanacearum* strains constitute a heterogeneous group subdivided into five races on the basis of their host range, six biovars based on their physiological and biochemical characteristics (Hayward, 2000), and four phylotypes according to phylogenetic information (Fegan and Prior, 2005; Remenant et al., 2010). Yamada et al. (2007), Yamada (2012) and Bhunchoth et al. (2015, 2016b) isolated and characterized various types of bacteriophages infecting *R. solanacearum* strains belonging to different races and/or biovars. Among them, ϕRP15, which was initially characterized as a myovirus with a wide host-range, replicates exclusively through a lytic cycle and forms clear plaques.

2. Results

2.1. Isolation and initial characterization of ϕRP15

ϕRP15 is a myovirus isolated in Pang Nga, Thailand (Bhunchoth et al., 2016b). It formed small clear plaques with a wide range of host strains (including those isolated in Japan). In contour-clamped homogeneous electric field (CHEF) gel electrophoresis analyses, the ϕRP15 genomic DNA produced a single band of approximately 170 kbp, being nearly the same size as the T4 genome (Fig. S1). An analysis of ϕRP15 particle morphology using electron microscopy revealed characteristics of a myovirus, with an icosahedral head (diameter: approximately 90 ± 5 nm, n = 10) and a long contractile tail (length: 110 ± 10 nm, n = 10; width: 18 ± 2 nm, n = 10) (Fig. 1). The tail consists of a T4-like neck with a collar and a sheath surrounding a tail tube or core. Remarkably, ϕRP15 particles show unique star-like protrusions stemming from the baseplate via a stalk, resembling the morphology shared by viunalikeviruses, but do not show prong-like structures attached to the baseplate as observed for viunalikeviruses (Adriaenssens et al., 2012a).

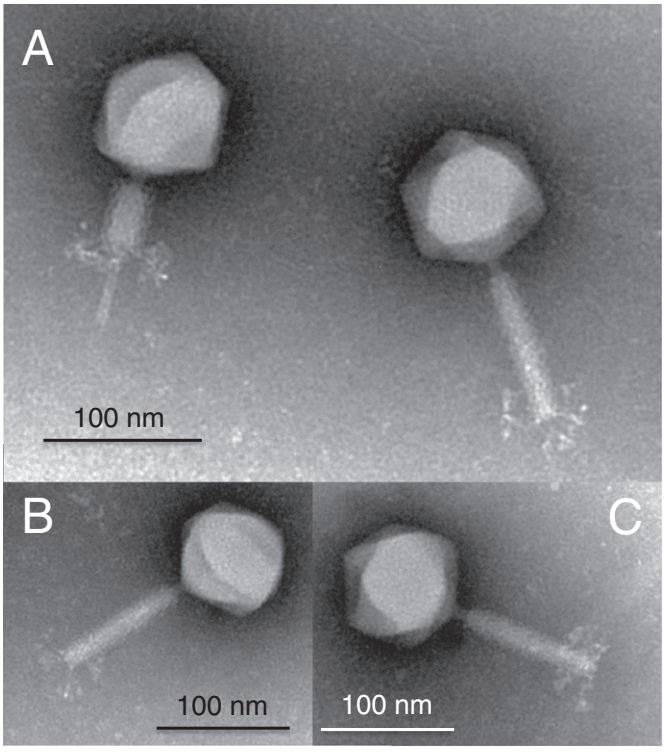

Fig. 1. Electron micrographs of ϕRP15 particles. Particles with contracted tail and uncontracted tail are compared (A). At the base plate region of uncontracted tail, umbrella-like (star-like) structures are obvious but no prong-like structures were visible (B and C). Particles were stained with 2% phosphotungstate.

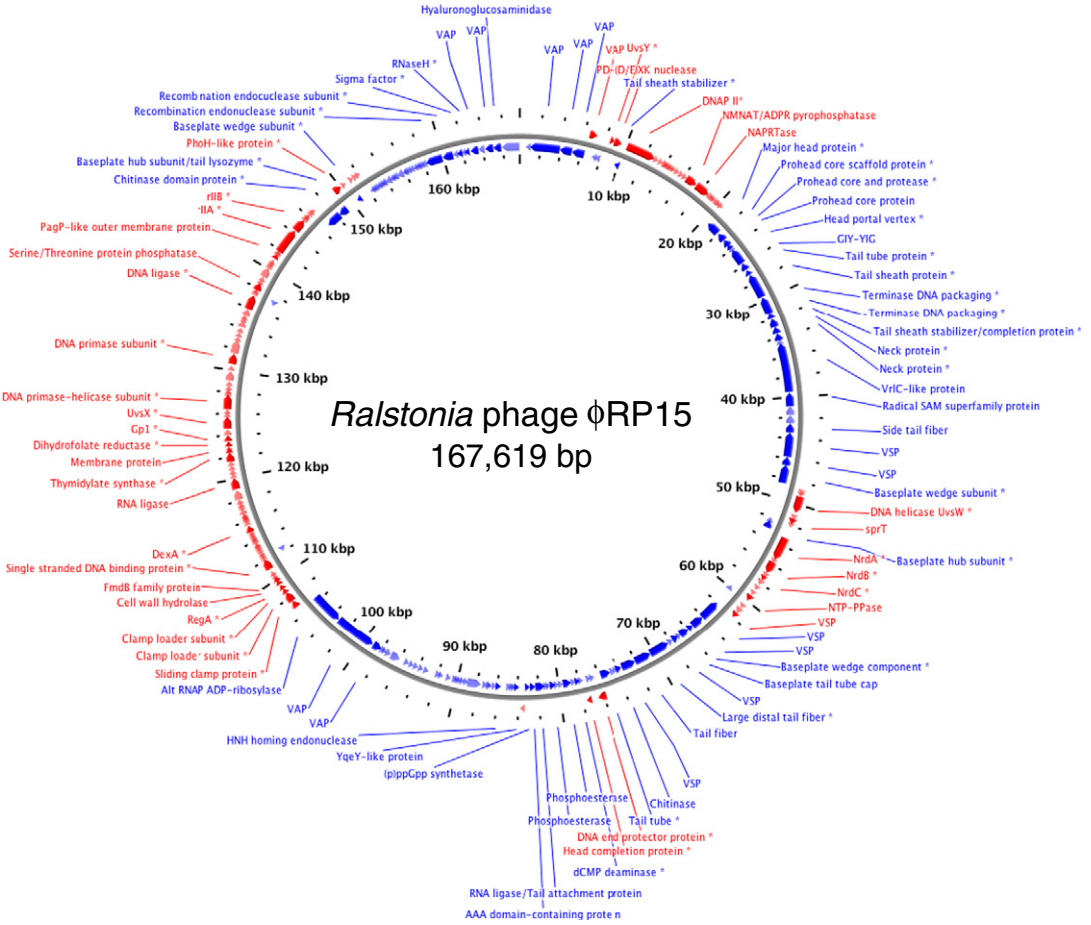

Fig. 2. Genome map of ϕRP15. Red arrows (forward) and blue arrows (reverse) indicates predicted ORFs. Asterisks indicate ORFs that are defined as the members of the T4 Core/Quasicore Genes.

2.2. General genomic features of ϕRP15

The nucleotide sequences of ϕRP15 were determined using shotgun sequencing of DNA purified from phage particles. The genomic sequences were assembled into a circular contig of 167,619 bp (accession no. LC121084). The ϕRP15 genomic DNA showed a G + C content of 44.7%, which was significantly lower than that of the host genomes (e.g., 66.97% for strain GMI1000; accession no. NC_003295). In total, 259 potential open reading frames (ORFs) (Fig. 2, Table S1) and seventeen tRNA genes (with two additional tRNA pseudogenes) were detected in the ϕRP15 genome. Approximately a half of the ϕRP15 ORFs (124/244, 50.8%) were located in a clockwise direction, with the remaining ORFs encoded in a counterclockwise direction. Based on similarities to biologically characterized proteins in sequence databases, 84 ORFs were functionally annotated. BLASTP searches against phage and viral genomes in the NCBI/RefSeq database revealed that 123 ϕRP15 ORFs showed significant sequence similarities to phage ORFs. Among the best hitting phages, *Delftia* phage ϕW-14, a T4-related phage, exhibited the largest number of best hits (36 out of 123; 29%).

2.3. Evolutionary relationships between ϕRP15 and T4-related phages

A previous study showed that *Delftia* phage ϕW-14 is phylogenetically related to viunalikeviruses. Examination of genomic similarities between ϕRP15, ϕW-14 and a viunalikevirus, *Dickeya* phage LIMEstone1, revealed long stretches of conserved genomic segments encoding many structural proteins between them (Fig. 3). Comparisons of ϕRP15 ORFs with the 37 "Core Genes (Petrov et al., 2010)" of T4-related phages revealed that ϕRP15 encodes 32 of the core genes (Table S2), indicating an evolutionary relationship between ϕRP15 and T4-related phages.

To further assess the genomic similarity between ϕRP15 and T4-related phages, we performed proteomic tree and phylogenetic tree reconstructions. A phage proteomic tree based on genome-wide sequence similarity scores revealed a clade containing 21 phages, which include ϕRP15, ϕW-14, viunalikeviruses and their close relatives (Fig. 4). Among these phages, ϕRP15 and ϕW-14 were found as a most deeply branching group. We also performed maximum likelihood phylogenetic tree reconstructions for

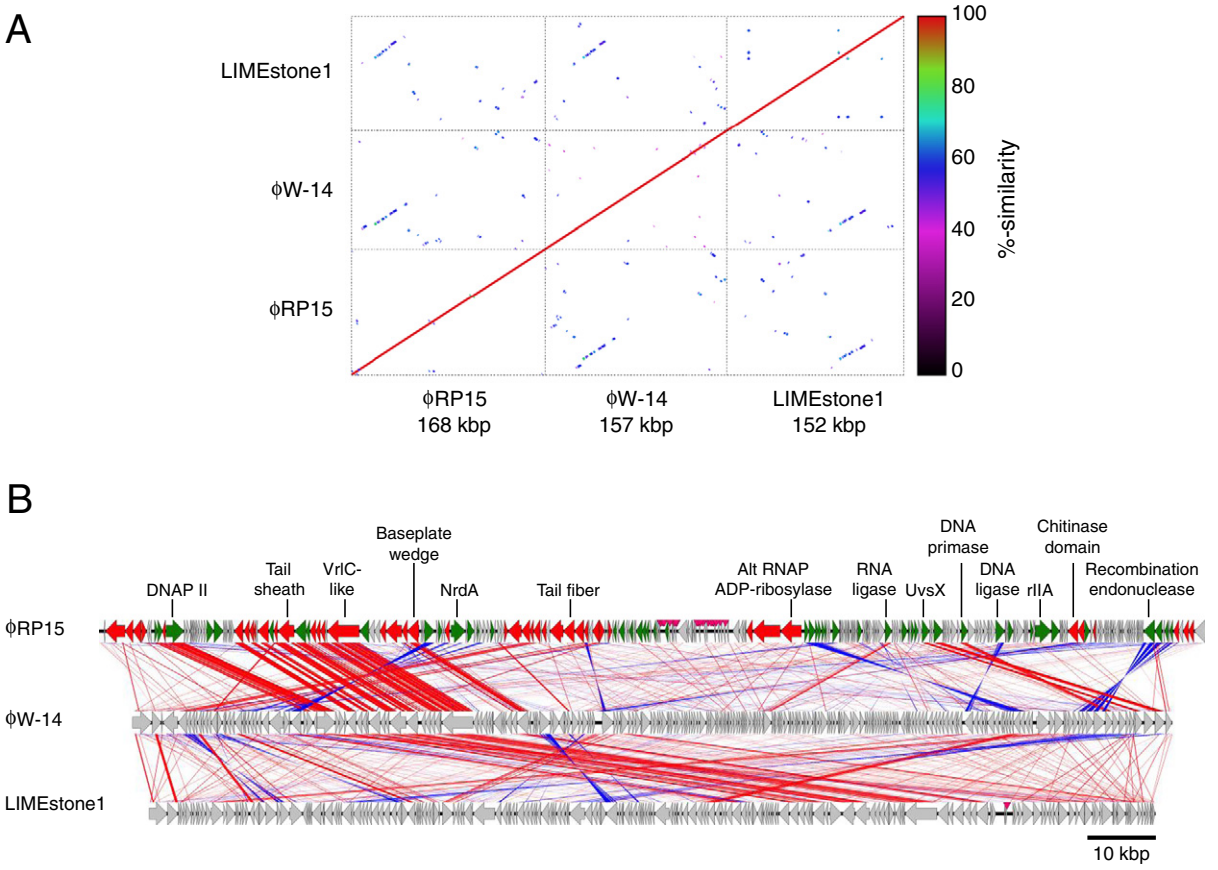

Fig. 3. Genome comparisons between ϕRP15, ϕW-14 and LIMEstone1. (A) Dot plot comparison generated using MUMmer 3.23/Promer, which compares six frame translations of the nucleotide sequences. The minimum length of a maximal exact match was set to 3. (B) Linear genome alignment highlighting conserved gene orders. The alignment was generated using Easyfig 2.2.2. Red arrows show structural protein coding ORFs of ϕRP15; green arrows, other functionally annotated ORFs of ϕRP15; and grey arrows, other ORFs. Red lines indicate TBLASTX matches (E-value < 10^{-8}) in the same direction along the genomes, while blue lines indicate inverted TBLASTX matches. Pink triangles indicate the positions of tRNA genes.

phage genes (tail sheath subunit, Fig. 5; DNA polymerase, Fig. S2A; DNA helicase, Fig. S2B; DNA primase-helicases, Fig. S2C; recombination endonuclease subunits, Fig. S2D). In all of the reconstructed phylogenetic trees, ϕRP15 and ϕW-14 formed a clade, which in turn is a sister group of the clade containing viunalikeviruses. Overall, the conservation of the "Core Genome" of T4-related phages and the proteomic and phylogenetic reconstructions suggest that ϕRP15 is a new member of T4-related phages closely related to ϕW-14 and viunalikeviruses.

2.4. ϕRP15 gene annotation

Here we describe notable genes found in the genomes of ϕRP15.

2.4.1. tRNAs and codon usage

The G + C content of the ϕRP15 genomic DNA (44.70%) was significantly lower than that of the host genome (ca. 67%). The gap between phage and host genomic nucleotide compositions (thus codon usage) may make it difficult for the phage to adapt to the host translation system. Some phages, especially lytic phages, are known to encode tRNA genes to solve this problem (Bailly-Bechet et al., 2007). There are 17 tRNAs (plus two pseudogenes) encoded in the ϕRP15 genome. They are located around a region at position 85,007 to 95,036 bp of the genome (Table S3). Codon usage was compared between host genes and phage genes (Table 1). Ten of these phage-encoded tRNAs corresponded to codons relatively abundant in the phage but rare in the host, while others (7/17) corresponded to codons highly used in both phage and host.

2.4.2. Nucleotide metabolism and DNA modification enzymes

ϕRP15 homologs of at least four characterized enzymes for deoxyribonucleotide triphosphate conversion and pyrimidine synthesis were detected in the ϕRP15 genome, including a thymidylate synthase (ORF164), a dihydrofolate reductases (ORF167), and

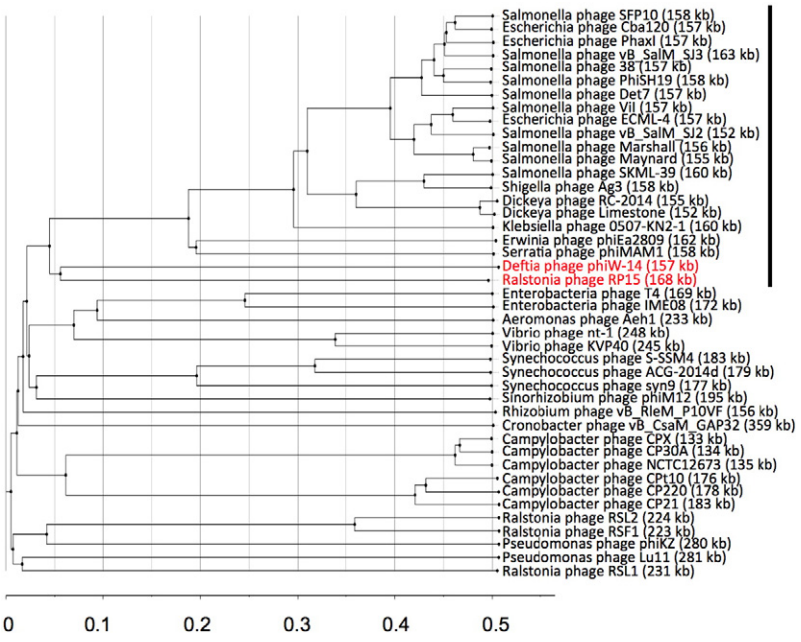

Fig. 4. Proteomic tree of ϕRP15 and other phages. The tree suggests a group of ϕRP15, ϕW-14, viunalikeviruses and their close relatives, as highlighted by a vertical line. The scale at the bottom indicates the TBLASTX-based proteomic distance d ($0 \le d \le 1$; (Bhunchoth et al., 2016a)) from the root.

aerobic ribonucleotide reductase subunits (ORF59 and ORF61). In addition, a deoxycytidylate deaminase (ORF89), a nucleotide pyrophosphatase (ORF67), a nicotinamide mononucleotide adenyltransferase (ORF21), and a nicotinamide phosphoribosyltransferase (ORF22) were encoded by ϕRP15. Contrasting to *Delftia* phage ϕW-14, ϕRP15 encodes no hydroxymethyluracyltransferase, which is responsible for substituting C for hydroxymethyluracil (HMdU). There were no homologs of enzymes involved in DNA modification,

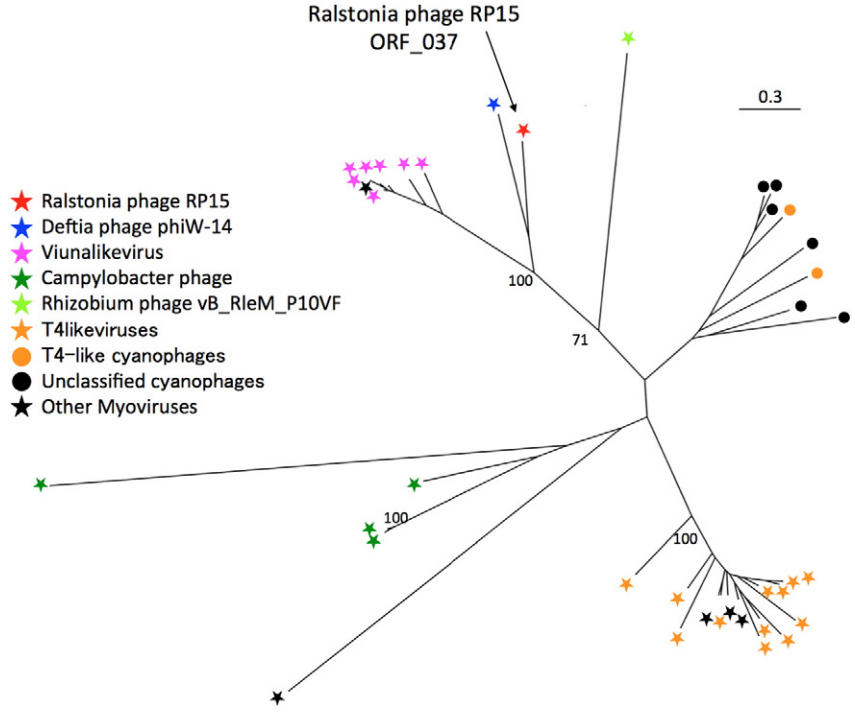

Fig. 5. Unrooted phylogenetic tree of Gp18 tail sheath subunit protein sequences from 39 phages including ϕRP15, ϕW-14, viunalikeviruses and other Myoviridae viruses. The tree was constructed with a maximum likelihood method with the LGF amino acid substitution matrix and the PROTGAMMA model. Bootstrap statistical supports (100 replicates) for nodes are given along the branches. The number on the scale bar indicates the number of substitutions per site. Identifiers for the sequences used in the tree are shown in Table S5.

Table 1
The codon usage and tRNA availability in RP15 and R. solanacearum (GMI1000).

Amino acid	Codon usage*				tRNA availability	
	Codon	Cumulative frequency per 10^3		Anticodon		
		R. solanacearum	RP15		*R. solanacearum*	RP15
Arg	CGU	5.3	15.9	ACG	1	
	CGC	47.8	8.4			
	CGA	2.2	3.6			
	CGG	15.2	5.7	CCG	1	
	AGA	0.7	7.4	UCU	1	1
	AGG	2.2	2.5	CCU	1	
Leu	UUA	0.3	0.5	UAA	1	
	UUG	6.3	19.3	CAA	1	1
	CUU	3	20.1			
	CUC	19.7	4.9	GAG	1	
	CUA	1.0	9.7	UAG	1	1
	CUG	73.3	20.9	CAG	2	
Ser	UCU	1.1	16.2			
	UCC	10.0	8.1	GGA	1	
	UCA	1.3	10.7	UGA	1	1
	UCG	20.9	7.6	CGA	1	
	AGU	1.7	8.0			
	AGC	18.0	8.6	GCU	1	1
Ala	GCU	5.1	23.5			
	GCC	63.4	15.1	GGC	2	
	GCA	9.1	24.7	UGC	4	
	GCG	56.0	9.8	CGC	1	
Gly	GGU	6.3	35.0			
	GGC	62.4	13.0	GCC	2	
	GGA	3.2	10.9	UCC	1	1
	GGG	11.1	11.4	CCC	1	
Pro	CCU	2.1	12.4			
	CCC	15.0	5.5	GGG	1	
	CCA	2.2	7.6	UGG	1	1
	CCG	34.7	11.9	CGG	1	
Thr	ACU	1.4	14.7			
	ACC	27.7	17.8	GGU	1	
	ACA	2.2	14.6	UGU	1	1
	ACG	23.5	11.8	CGU	1	
Val	GUU	3.3	29.5			
	GUC	26.8	11.9	GAC	1	
	GUA	1.9	7.7	UAC	1	
	GUG	42.9	19.6	CAC	1	
Ile	AUU	4.4	34.5			
	AUC	38.4	27.4	GAU	4	1
	AUA	0.6	0.8			
Asn	AAU	4.9	30.0			
	AAC	21.6	25.2	GUU	1	1
Asp	GAU	15.2	45.2			
	GAC	38.4	19.4	GUC	3	
Cys	UGU	0.8	5.2			
	UGC	8.5	4.3	GCA	2	
Gln	CAA	5.6	21.7	UUG	1	1
	CAG	33.2	14.1			
Glu	GAA	17.8	45.8	UUC	2	
	GAG	31.6	20.7			
His	CAU	7.1	11.6	GUG	1	
	CAC	16.4	5.5			
Lys	AAA	3.7	23.1	UUU	1	1
	AAG	25.0	47.7	CUU	1	
Phe	UUU	4.3	20.0			
	UUC	29.2	27.0	GAA	1	1
Tyr	UAU	6.2	27.3			
	UAC	17.1	14.8	GUA	1	1
Met	AUG	23.0	27.4	CAU	4	2
Trp	UGG	14	13.8	CCA	1	1

* The total no. of codons are 1,692,068 for *R. solanacearum* GMI1000 (5083 protein-coding genes, accession nos. AL646052 and AL646053) and 49,577 for ϕRP15 (259 genes), respectively.

such as adenine and cytosine methylation or cytosine hydroxymethylation, in either genome. The presence of ORFs related to DNA-methyltransferases could not be confirmed.

2.4.3. Lysis and host-phage interaction

Four ϕRP15 ORFs showed amino acid sequence similarities to cell lytic enzymes. ORF81 showed similarity to the *Pseudomonas* chitinase (A6A037W170, E-value = 5.00E−73). ORF133 and ORF207 were similar to cell wall hydrolases (C9DFZ4, 4.00E−35) and chitinase (C9DG53, 1.00E−52 of *Delftia* phage ϕW-14), respectively. ORF208 encodes a tail lysozyme (K7YB77, 1.00E−27). The last one was a structural protein (see below) likely involved in phage-host interaction. Protein products of ORF81 and ORF207 were also detected in virions (Fig. 6). Chitinase digests polymers of β-linked *N*-acetylglucosamine and may be involved in biofilm degradation upon infection. In addition, ORF243 encoding a hyaluronoglucosaminidase was also virion-associated and is likely involved in host polysaccharide degradation.

2.4.4. Structural proteins

A comparative analysis of the ϕRP15 genome sequence enabled the initial annotation of 34 virion-associated protein genes (Table S1). These include genes for structural proteins such as a tail tube protein (ORF36), neck proteins (ORF41, and ORF42), a major capsid protein (ORF29), a prohead core protein (ORF30), a prohead core scaffolding protein (ORF31), a portal vertex protein (ORF34), a tail sheath protein (ORF37), a tail sheath stabilizer protein (ORF40), baseplate wedge proteins (ORF51 and ORF73), a base plate (ORF58), a baseplate tube cap protein (ORF74), a large distal tail fiber protein (ORF78), a tail fiber protein (ORF79), a tail tube monomer (ORF84), a head completion protein (ORF87), a sliding clamp (ORF129), clamp loader proteins (ORF130 and ORF131), a baseplate hub subunit and tail lysozyme (ORF208), a baseplate wedge subunit (ORF211) and other possible structural

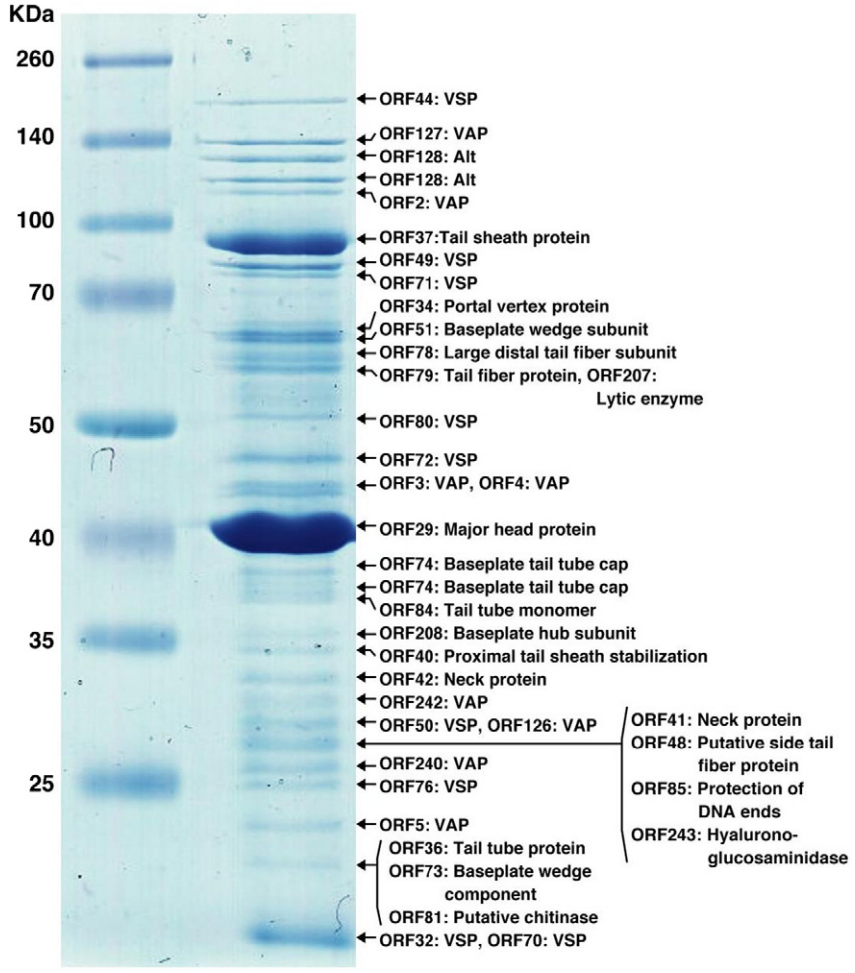

Fig. 6. Proteomic analysis of virion proteins of ϕRP15. Virion proteins separated by SDS-PAGE were visualized with Coomassie Brilliant Blue (lane 2). Molecular size marker was a Spectra Multicolor Protein Ladder (Thermo Fisher Scientific KK., Yokohama, Japan). The protein bands were excised from the gel, digested with trypsin, and analyzed by liquid chromatography-tandem mass spectrometry (LTQ Orbitrap XL). Assignment of tandem mass spectrometry data to tryptic peptides encoded by phage open reading frames was completed using an established procedure (Bhunchoth et al., 2016a). VAP: virion associated protein. VSP: virion structural protein. The number of unique identified peptides and the corresponding protein sequence coverage ranges are listed in Table 2.

Table 2
Mass spectrometry data for RP15 virion proteins.

Gel band	Gene annotation/ORF	Protein name	Obs. mol. mass (kDa)	Theo. mol. mass (kDa)	No. of unique peptides	Protein sequence coverage (%)	Mascott score
1	RP15_044	VrlC-like protein	190	178.75	46	22.17	1178.47
2	RP15_127	Virion associated protein	140	152.38	43	23.53	1011.12
3	RP15_128	Alt RNA polymerase ADP-ribosylase	130	117.09	26	22.83	830.9
4	RP15_128	Alt RNA polymerase ADP-ribosylase	120	117.09	36	28.08	1025.4
5	RP15_002	Virion associated protein	115	107.49	30	32.00	1034.36
6	RP15_037	Tail sheath protein	95	90.16	66	55.69	5426.89
7	RP15_049	Virion structural protein	85	86.00	33	31.83	1698.59
8	RP15_071	Virion structural protein	80	73.22	24	21.57	679.11
9	RP15_034	Portal vertex protein of head	65	62.40	36	41.54	1339.57
10	RP15_051	Baseplate wedge subunit	63	65.82	47	52.53	3266.89
11	RP15_078	Large distal tail fiber subunit	61	69.47	12	22.04	1854.24
12	RP15_079	Tail fiber protein	58	56.99	8	12.05	340.17
12	RP15_207	Chitinase domain protein	58	53.71	7	10.87	127.31
13	RP15_080	Virion structural protein	50	49.95	3	5.73	108.81
14	RP15_072	Virion structural protein	47	48.27	6	12.35	195.35
15	RP15_003	Virion associated protein	44	41.37	9	28.89	592.64
15	RP15_004	Virion associated protein	44	46.43	8	16.46	252.49
16	RP15_029	Major head protein	41	47.02	34	69.53	12,996.68
17	RP15_074	Baseplate tail tube cap	38	36.13	18	47.55	664
18	RP15_074	Baseplate tail tube cap	37.5	36.13	9	23.62	194.14
19	RP15_084	Tail tube monomer	37	36.42	8	17.23	225.93
20	RP15_208	Baseplate hub subunit and tail lysozyme	35	33.71	10	21.79	370.88
21	RP15_040	Proximal tail sheath stabilization	34	32.70	8	27.21	414.16
22	RP15_042	gp13 Neck protein	32	29.43	6	20.87	232.55
23	RP15_242	Virion associated protein	31	27.72	5	8.71	138.67
24	RP15_050	Virion structural protein	29	31.76	10	29.21	376.43
24	RP15_126	Virion associated protein	29	33.07	21	41.22	933.58
25	RP15_041	gp14 Neck protein	28	26.07	11	32.89	489.35
25	RP15_048	Putative side tail fiber protein	28	30.45	7	25.17	399.2
25	RP15_085	gp2 Protection of ends of packaged DNA	28	30.43	16	36.19	424.68
25	RP15_243	Hyaluronoglucosaminidase	28	27.91	11	25.48	471.55
26	RP15_240	Virion associated protein	26	28.56	10	38.43	423.69
27	RP15_076	Virion structural protein	25	21.20	10	60.29	1011.96
28	RP15_005	Virion associated protein	24	28.27	7	14.00	116.55
29	RP15_036	gp19 Tail tube protein	23	19.57	3	12.57	97.13
29	RP15_073	gp53 Baseplate wedge component	23	21.90	3	10.27	37.9
29	RP15_081	Putative chitinase	23	22.43	1	3.94	40.65
30	RP15_032	Virion structural protein	22	10.53	1	9.78	62.78
30	RP15_070	Virion structural protein	22	19.95	2	11.43	99.84

The proteins detected by MS are listed with their theoretical molecular mass and observed molecular mass (from SDS PAGE). The number of identified peptides in each protein and the corresponding protein sequence coverage are indicated.

proteins. Reversed-phase nano-liquid chromatography directly coupled with liquid chromatography-tandem mass spectrometry analysis of ϕRP15 virion proteins separated by sodium dodecyl sulfate polyacrylamide gel electrophoresis (SDS-PAGE) resulted in the identification of 37 ϕRP15 virion proteins (Fig. 6, Table 2). These included 28 of the 34 ϕRP15 ORFs (82%) that were predicted to be virion-associated based on homology searches plus additional nine proteins showing marginal homology to some enzymes and other unknown proteins (finally annotated as virion-structural or -associated proteins). Genes encoding the structural proteins formed clusters on the ϕRP15 genomic map (Fig. 2). Contrasting to members of the *Viunalikevirus*, tail spike proteins were not detected in the ϕRP15 virion. Tail spike genes are encoded within a conserved genomic region of *Viunalikevirus* phages (Adriaenssens et al., 2012a), but they are missing in the ϕRP15 genome.

2.4.5. Mobile elements

Homing endonucleases are mobile genetic elements and are suggested to confer a selective mobility of the flanking sequences in the phage genome (Goodrich-Blair and Shub, 1996). As many as 15 homing endonucleases were reported for T4 phage (Edgell et al., 2010). In the ϕRP15 genome, two such genes were detected. ORF35 encodes a GIY-YIG endonuclease embedded in a

possible structural module consisting of 23 ORFs (ORF29-ORF51) (Fig. 2). ORF104 encoding an HNH endonuclease was located adjacent to the large cluster of tRNA genes (Table S1).

2.4.6. Other genes

Other ϕRP15 ORFs with putative functional annotations include an arylsulfatase regulator AslB (ORF45), a SprT-like Zinc-metallopeptidase (ORF55), a RelA/SpoT family (p)ppGpp synthase (ORF99), an Alt ADP-ribosyltransferase (ORF128), a metallophosphatases (ORF192), an HSP90 family protein (ORF201), a PhoH-like protein (ORF209) (Table S1). The actual expression patterns and functions of these gene products during the phage infection cycle are unknown. Protein bands corresponding to the Alt ADP-ribosyltransferase (ORF128) were detected in the ϕRP15 virions (Fig. 6). Alt ADP-ribosyltransferase is known in T4 to be introduced into the host cells for modification of host proteins, especially the α-subunit of RNA polymerase for possible modification of phage early transcription (Rohrer et al., 1975). As many as 27 target proteins ADP-ribosylated by T4 Alt were detected and suggested to be involved in the rapid shift of gene expression from host to phage (Depping et al., 2005).

2.5. ϕRP15 infection cycles

The ϕRP15 infection cycle was examined using single-step growth experiments with *R. solanacearum* strain MAFF 730138 as the host. As shown in Fig. 7A, ϕRP15 infection proceeded efficiently. One infection cycle took 100 min with a latent period of 60 min. The burst size was approximately 80 plaque-forming units (pfu)/cell. Results of adsorption experiments showed a standard pattern (Fig. 7B) with a rate constant (k) 4.6×10^{-9} cm^3/min, comparable with T-even phages (Kasman et al., 2002). This adsorption efficiency was much lower than LIMEstone1 and LIMEstone2 (typical viunalikeviruses), for both of which >99.9999% of phages were irreversibly adsorbed to the host cells within 1 min (Adriaenssens et al., 2012b). In the case of ϕRP15 adsorption, approximately 10% of adsorbed phage particles were reversibly released from the cell at 10 min after infection, while 30% of adsorbed phages were still reversibly released from the host cells in the case of ϕRSL1 (Yamada et al., 2010) (Fig. 7C). Therefore, ϕRP15 adsorption was relatively stable.

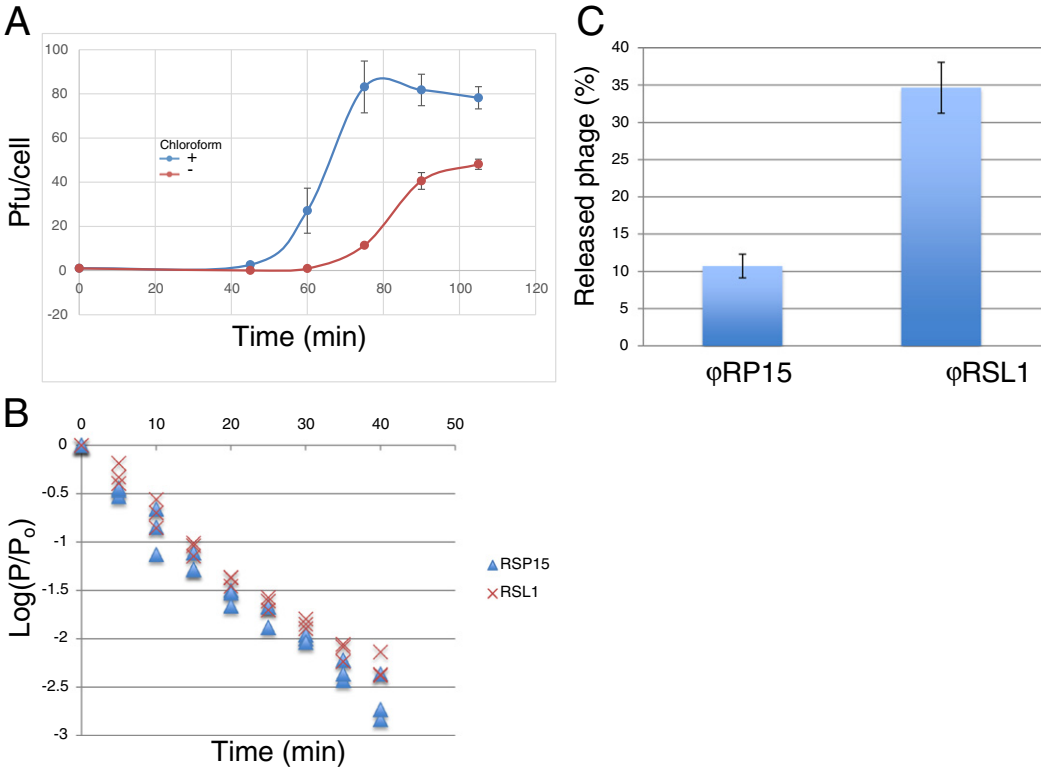

Fig. 7. Single-step growth (A), adsorption (B) and phage release (C) assays of ϕRP15. The single-step growth curves indicated that the latent period, one infection cycle, and burst size of ϕRP15 are 60 min, 100 min, 80 pfu/cell, respectively (A). Without chloroform treatment, phage titer was decreased, indicating incomplete cell lysis. From the adsorption curve (B), the adsorption constant k [$k = 2.3 / (N \times t) \times \log(P_0 / P)$] was calculated to be 4.6×10^{-9} cm^3/min. Data of three independent experiments were plotted. For comparison, experiments with ϕRSL1 were paralleled (×). For assays of reversibly released phages, the precipitate after centrifugation was resuspended by vortexing for 30 s in 500 μl CPG. Released phages (%) from the host at 10 min post infection was ca. 10% and ca. 35% for ϕRP15 and ϕRSL1(control), respectively (C). In each assays, standard deviations were calculated from three independent experiments.

3. Discussion

3.1. ϕRP15 and Viunalikevirus phages

From our proteomic and phylogenetic tree analyses, ϕRP15 was found to be evolutionarily related to phages of viunalikeviruses. The genus *Viunalikevirus* is characterized by a unique virion morphology, a conserved genome organization, horizontally acquired tRNA genes and the possible substitution of an alternate base for thymine in the DNA (Adriaenssens et al., 2012a). Morphological peculiarity of viunalikeviruses includes a series of unique protrusion stemming from the base plate; 3 to 4 thick rounded prongs (located at the bottom of the base plate) and an equal number of thinner star-like protrusions attached to the base plate via a stalk. The ϕRP15 virions observed by EM showed different figures (Fig. 1). Although protrusions attached to the side of the base plate were obvious (showing star-like or umbrella-like structures), no prong-structure was visible at the bottom of the base plate. The tail spike region in viunalikevirus genomes always contains a tandem array of distinct genes for tail spike proteins (Adriaenssens et al., 2012a), while no such genes were identified in the ϕRP15 genome (Table S1) and no spike proteins were detected in the virion proteome analyses (Fig. 6). Therefore, such tail spike proteins may be responsible for the prong structures in viunalikeviruses and in this respect, ϕRP15 is different from canonical members of the genus *Viunalikevirus*. Related with this structural difference, it would be interesting to point out that attachment of ϕRP15 to the host cells occurred with efficiency comparable with T-even phages (Fig. S2) but LIMEstone phages adsorb much more efficiently to the host cells (Adriaenssens et al., 2012b). Therefore, the prong-structures specifically observed for viunalikeviruses are likely involved in rapid and stable adsorption of phages to the host (Adriaenssens et al., 2012a). Once adsorbed, release of ϕRP15 particles from the host cells was relatively rare, so that the star-like structure may be responsible for the irreversible adsorption.

In the phylogenetic trees (Fig. 5, Fig. S2), ϕRP15 forms a clade with *Delftia* phage ϕW-14 branched from the root of the *Viunalikevirus* clade. The ϕW-14 genome is 157,486 bp long, containing 237 genes (accession no. GQ357915). This genome is approximately 10 kbp smaller than that of ϕRP15 and lacks a region containing tRNAs. This contrasts with the ϕRP15 genome that contains as many as 19 tRNA-related sequences. Typically, members of *Viunalikevirus* encode 1 to 6 tRNA genes. ϕRP15 and ϕW-14 thus represent both extreme cases. *Delftia* phage ϕW-14 is known as a phage containing a peculiar modified base in the genome (Kropinski et al., 1973). Half of the thymine residues are replaced with α-putrescinylthymine (putThy). Thymine and putThy are formed from hydroxymethyl uracil (HMdU). A gene for hydroxymethyluracil transferase is encoded in ϕW-14, while it is missing in the ϕRP15 genome and also in vinualikeviruses. However, it was suggested that thymidylate synthases encoded by most viunalikeviruses are closely related to the HMdU transferase (Adriaenssens et al., 2012a). Occurrence of HMdU in the ϕRP15 genome is unlikely, because most restriction enzymes (16 different enzymes) digested this DNA with no exception (data not shown). From these results, ϕRP15 and ϕW-14 represent a lineage independent from *Viunalikevirus*. It is noteworthy to point out that hosts of ϕRP15 and ϕW-14 (*R. solanacearum* and *Delftia acidovorans*, respectively) belong to Betaproteobacteia, while most hosts of viunalikeviruses known to date are of *Enterobacteriaceae* belonging to Gammaproteobacteria. These phages may have evolved in close association with their hosts that have very different life-styles in the natural habitats.

In natural environments, soil-borne *R. solanacearum* cell growth is essentially saprophytic but becomes phytopathogenic under special circumstances when the bacterium comes into contact with plants (Hayward, 1991). In such complex life cycles, bacterial cells interact with various kinds of phage. In addition to known *Ralstonia* phages such as inoviruses (ϕRSM, ϕRSS, etc.), podoviruses (ϕRSB, ϕRSJ, etc.), siphoviruses (ϕRSC), (Yamada, 2012) and myoviruses including P2-like phage (ϕRSA1 and ϕRSX) (Fujiwara et al., 2008), ϕKZ-like phages (ϕRSL2 and ϕRSF1) (Bhunchoth et al., 2016a), and ϕRSL1-like phage (Yamada et al., 2010), a new myovirus group represented by ϕRP15 has been characterized in this work.

4. Materials and methods

4.1. Bacterial strains, bacteriophages, and culture conditions

The *R. solanacearum* strains used in this study, along with their hosts and taxonomic features, are listed in Table S4. The bacterial cells were cultured in CPG medium containing 0.1% (w/v) casamino acids, 1.0% (w/v) peptone, and 0.5% (w/v) glucose (Horita and Tsuchiya, 2002) at 28 °C with shaking at 200–300 rpm. For long-term storage, bacterial cultures were kept in sterile 20% (v/v) glycerol at −80 °C. Bacteriophage ϕRP15 was isolated from tomato fields in Pang Nga, Thailand using an established isolation procedure (Bhunchoth et al., 2016b). Briefly, 1 g soil was suspended in 2 ml distilled water and vigorously shaken for 1 h at room temperature to release bacteriophages. The mixture was filtered through a membrane filter (0.45-μm pore; Pall Corporation, NY, USA). The suspension (100 μl aliquots) was used in a plaque-forming assay, with *R. solanacearum* MAFF 730138 as the host, on CPG plates containing 1.5% agar overlaid with 0.45% CPG soft agar. Phage was routinely propagated using *R. solanacearum* strain MAFF 730138 as the host. When the cultures reached an OD_{600} of 0.5, bacteriophages were added at a multiplicity of infection of 0.01–0.1. After culturing for a further 12–24 h, the cells were removed by centrifugation at 8000 $\times g$ for 15 min at 4 °C. The supernatant was filtered (0.45 μm membrane), and the pellet was dissolved in SM buffer (50 mM Tris-HCl at pH 7.5, 100 mM NaCl, 10 mM $MgSO_4$, and 0.01% gelatin). For further purification, the phage suspension was layered on a 20–60% sucrose gradient and centrifuged at 40,000 $\times g$ for 1 h. The purified phages were stored at 4 °C. The phage particles were stained with 2% Na-phosphotungstate or 2% uranyl acetate and analyzed using a JEOL JEM-1400 electron microscope

(JEOL Ltd., Tokyo, Japan) according to the method of Dykstra (1993). We used λ phage particles as an internal standard marker for size determination.

4.2. Single-step growth experiments and adsorption assays

Single-step growth experiments were performed as previously described (Yamada et al., 2010), with some modifications. Strain MAFF 730138 was used as the host. Bacterial cells (0.1 U of OD_{600}) were harvested by centrifugation at 8000 ×*g* for 15 min at 4 °C and resuspended in fresh CPG medium (approximately 1×10^8 colony-forming units/ml) in a final volume of 10 ml. The phage was added at a multiplicity of infection (MOI) of 0.1 and allowed to adsorb for 10 min at 28 °C. After centrifugation at 8000 ×*g* for 15 min at 28 °C, samples were resuspended using the initial volume of CPG, and serial dilutions were prepared in a final volume of 10 ml. The cells were incubated at 28 °C. Samples were removed at 30-min intervals up to 5 h and the titers were determined with or without chloroform treatment using double-layered agar plates. In adsorption experiments, the host cells (strain MAFF 730138) were grown to an OD_{600} of 0.1 (5 ml) and infected with phages at MOI of 0.1. Immediately after infection, a 500 μl sample was taken and centrifuges at 10,000 ×*g* for 1 min at 28 °C. The supernatant was filtrated through a membrane filter (0.45-μm pore size, Steradisc, Krabo Co. Ltd. Osaka, Japan) and titrated to determine the amount of non-adsorbed (or reversibly adsorbed) phages. This was repeated at 5, 10, 20, 25, 30, 35, and 40 min post infection. For assays of reversibly released phages at 10 min post infection, the precipitate after centrifugation was resuspended by vortexing for 30 s in 500 μl CPG at 0 °C and centrifuged (10,000 ×*g* for 1 min at 28 °C). The supernatant was filtrated as above and subjected to plaque-forming assays.

4.3. Isolation and characterization of genomic DNA from phage particles

Standard techniques for DNA isolation, digestion with restriction enzymes, construction of recombinant DNA, and sequencing were completed according to Sambrook and Russell (2001). Genomic DNA was isolated from the purified phage particles by phenol extraction. To determine genome size, the purified phage particles were embedded in 0.5% low-melting-point agarose (InCert agarose, FMC Corp., Philadelphia, PA, USA). Following treatment with proteinase K (1 mg/ml; Merck Ltd., Tokyo, Japan) and 1% (w/v) sarkosyl, the nucleic acids were subjected to pulsed-field gel electrophoresis using the CHEF Mapper electrophoresis apparatus (Bio-Rad, Hercules, CA, USA) as described by Higashiyama and Yamada (1991). Shotgun sequencing of phage genomic DNA was completed at Hokkaido System Science Co., Ltd. (Sapporo, Japan) using a Roche GS Junior System. Draft sequences were assembled using GS De Novo Assembler, version 2.6. The analyzed sequences corresponded to 600 times the final contig sizes of ϕRP15 (167,619 bp).

4.4. Bioinformatics

Potential ORFs longer than 90 bp (30 codons; ATG, GTG, TTG and CTG starts) were identified using Glimmer, version 3.02 (Delcher et al., 1999). Homology searches were performed using BLASTP/RPS-BLAST (Altschul et al., 1997) tools against NCBI/Cdd sequence domain database (version 3.14, Wheeler et al., 2007), UniProt sequence database (Uniprot Consortium, 2014), and NCBI RefSeq complete viral genome database (Release 74). An E-value lower than 1e−5 was used as the cutoff for notable similarity. tRNA genes were identified using tRNAScan-SE 1.4 (option: —B for bacterial tRNAs) (Lowe and Eddy, 1997). T4 "Core Genes" were identified using PSI-BLAST from T4 genes as well as BLASTP from ϕRP15 against RefSeq. Circular genome maps were generated using CGView (Stothard and Wishart, 2005) and dot-plots by MUMmer 3.23 (Kurtz et al., 2004). Sequences were aligned using MAFFT v6.861b (Katoh and Toh, 2008) with default parameters. Accession numbers for the sequences used in the alignments are given in Table S5. Alignments were trimmed using trimAl v1.4.rev6 (Capella-Gutiérrez et al., 2009) if it improved the trees. Model of protein evolution were selected using ProtTest (Abascal et al., 2005) as implemented in *pmodeltest* v1.4. Tree reconstruction was performed using RaxML v8.1.20 (Stamatakis, 2014) with the selected model and PROTGAMMA parameter. Branch supports were drawn from 100 bootstrap replicates. Viral proteomic tree was constructed as previously described (Bhunchoth et al., 2016a).

4.5. Identification of in-gel digested proteins by liquid chromatography-tandem mass spectrometry

Purified phage particles were subjected to SDS-PAGE [10–12% (wt/vol) polyacrylamide] according to the method of Laemmli (1970). Protein bands excised from the gel were digested with trypsin after reduction with dithiothreitol and alkylation with iodoacetamide. After trapping with a short ODS column (PepMap 100; 5 μm C18, 5 mm × 300 μm ID; Thermo Fisher Scientific Inc., Waltham, MA, USA), tryptic peptides were separated with another ODS column (Nano HPLC Capillary Column; 3 μm C18, 120 mm × 75 μm ID; Nikkyo Technos, Tokyo, Japan) using nano-liquid chromatography (Ultimate 3000 RSLC nano system; Thermo Fisher Scientific). The elution condition was the same as previously described (Bhunchoth et al., 2016a). The eluate from the separation column was continuously introduced into a nanoESI source and analyzed by mass spectrometry (MS) and MS/MS (LTQ Orbitrap XL; Thermo Fisher Scientific) at the Natural Science Center for Basic Research and Development, Hiroshima University. The MS and MS/MS spectra were generated in the positive ion mode using Orbitrap (mass range: *m/z* 300 to 1500) and Iontrap (data-dependent scan of the top five peaks using CID), respectively. The voltage of the capillary source was set at 1.5 kV, and the temperature of the transfer capillary was maintained at 200 °C. The capillary voltage and tube lens voltage were set at 20 V and

80 V, respectively. The assignment of the MS/MS data to tryptic peptides encoded by phage ORFs was completed as previously described (Bhunchoth et al., 2016a) using the Xcalibur program, version 2.0 (Thermo Fisher Scientific). All MS/MS data were searched using Mascot (Matrix Sciences) against the GeneBank non-redundant protein database and against a local database of all possible ϕRP15 gene products using Proteome Discoverer software (ver. 1.4, Thermo Scientific). Doubly, triply and quadruply charged peptide ions were subjected to the database search with a parent and peptide ion mass tolerance of ±10 ppm and ±0.8 Da, respectively. Possible static and chemical modifications included were cysteine carbamidomethylation, methionine oxidation and deamidation of asparagine and glutamine. The significance threshold on Proteome Discoverer for Mascot search was set at $P < 0.05$ and one and two missed trypsin cleavage was allowed.

Supplementary data to this article can be found online at http://dx.doi.org/10.1016/j.virep.2016.07.001.

Conflict of interest

The authors have no conflicts of interest to declare.

Acknowledgments

This study was supported by the Strategic Japanese-Thai Research Cooperative Program (SICP) on Biotechnology (JST/BIOTEC-SICP). TY and HO were partially supported by JSPS KAKENHI (grant numbers 24380049 and 26430184, respectively). Some of the computational work was completed at the SuperComputer System, Institute for Chemical Research, Kyoto University.

References

Abascal, F., Zardoya, R., Posada, D., 2005. ProtTest: selection of best-fit models of protein evolution. Bioinformatics 21, 2104–2105.
Adriaenssens, E.M., Ackermann, H.-W., Anany, H., Blasdel, B., Connerton, I.F., Goulding, D., Griffiths, M.W., Hooton, S.P., Kutter, E.M., Kropinski, A.M., Lee, J.-H., Maes, M., Pickard, D., Ryu, S., Sepehrizadeh, Z., Sharbabak, S.S., Tribio, A.L., Lavigne, R., 2012a. A suggested new bacteriophage genus: "*Viunalikevirus*". Arch. Virol. 157, 2035–2046.
Adriaenssens, E.M., Van Vaerenbergh, J., Vandenheuvel, D., Dunon, V., Ceyssens, P.J., De Proft, M., Kropinski, A.M., Noben, J.-P., Maes, M., Lavigne, R., 2012b. T4-related bacteriophage LIMEstone isolates for the control of soft rot on potato caused by '*Dyckeya solani*'. PLoS One 3, e33227.
Altschul, S.F., Madden, T.L., Schaffer, A.A., Zhang, Z., Miller, W., Lipman, D.J., 1997. Gapped BLAST and PSI-BLAST: a new generation of protein database search programs. Nucleic Acids Res. 25, 3389–3402.
Bailly-Bechet, M., Vergassola, M., Rocha, E., 2007. Causes for the intriguing presence of tRNAs in phages. Genome Res. 17, 1486–1495.
Bhunchoth, A., Phironrit, N., Leksomboon, C., Chatchawankanphanich, O., Kotera, S., Narulita, E., Kawasaki, T., Fujie, M., Yamada, T., 2015. Isolation of *Ralstonia solanacearum*-infecting bacteriophages from tomato fields in Chiang Mai, Thailand, and their experimental use as biocontrol agents. J. Appl. Microbiol. 118, 1023–1033.
Bhunchoth, A., Blanc-Mathieu, R., Mihara, T., Nishimura, Y., Askora, A., Phironrit, N., Leksomboon, C., Chatchawankanphanich, O., Kawasaki, O., Nakano, M., Fujie, M., Ogata, H., Yamada, T., 2016a. Two Asian jumbo phages, ϕRSL2 and ϕRSF1, infect *Ralstonia solanacearum* and show common features of ϕKZ-related phages. Virology 494, 56–66.
Bhunchoth, A., Phironrit, N., Leksomboon, C., Kawasaki, T., Yamada, T., Chatchawankanphanich, O., 2016b. Isolation and characterization of bacteriophages infecting *Ralstonia solanacearum* in Thailand. Acta Hortic. (in press).
Capella-Gutiérrez, S., Silla-Martínez, J.M., Gabaldón, T., 2009. trimAl: a tool for automated alignment trimming in large-scale phylogenetic analyses. Bioinformatics 25, 1972–1973.
Delcher, A.L., Harmon, D., Kasif, S., White, O., Salzberg, S.L., 1999. Improved microbial gene identification with GLIMMER. Nucleic Acids Res. 27, 4636–4641.
Depping, R., Lohaus, C., Meyer, H.E., Rüger, W., 2005. The mono-ADP-ribosyltransferases Alt and ModB of bacteriophage T4: target proteins identified. Biochem. Biophys. Res. Commun. 335, 1217–1223.
Dykstra, M.J., 1993. A Manual of Applied Technique for Biological Electron Microscopy. Plenum Press, New York.
Edgell, D.R., Gibb, E.A., Belfort, M., 2010. Mobile DNA elements in T4 and related phages. Virol. J 7, 290.
Fegan, M., Prior, P., 2005. How complex is the "*Ralstonia solanacearum* species complex"? In: Allen, C., Prior, P., Hayward, A.C. (Eds.), Bacterial Wilt Disease and the *Ralstonia solanacearum* Species Complex. APS Press, St. Paul, pp. 449–461
Filee, J., Bapteste, E., Susko, E., Krisch, H.M., 2006. A selective barrier to horizontal gene transfer in the T4-type bacteriophages that has preserved a core genome with the viral replication and structural genes. Mol. Biol. Evol. 23, 1688–1696.
Fujiwara, A., Kawasaki, T., Usami, S., Fujie, M., Yamada, T., 2008. Genomic characterization of *Ralstonia solanacearum* phage ϕRSA1 and its related prophage (ϕRSX) in strain GMI1000. J. Bacteriol. 190, 143–156.
Goodrich-Blair, H., Shub, D.A., 1996. Beyond homing: competition between intron endonucleases confers a selective advantage on flanking genetic markers. Cell 84, 211–221.
Hayward, A.C., 1991. Biology and epidemiology of bacterial wilt caused by *Pseudomonas solanacearum*. Annu. Rev. Phytopathol. 29, 65–87.
Hayward, A.C., 2000. Ralstonia solanacearum. In: Lederberg, J. (Ed.), Encyclopedia of Microbiology vol. 4. Academic Press, San Diego, CA., pp. 32–42.
Hendrix, R.W., 2009. Jumbo bacteriophages. Curr. Top. Microbiol. Immunol. 328, 229–240.
Higashiyama, T., Yamada, T., 1991. Electrophoretic karyotyping and chromosomal gene mapping of *Chlorella*. Nucleic Acids Res. 19, 6191–6195.
Horita, M., Tsuchiya, K., 2002. Causal agent of bacterial wilt disease *Ralstonia solanacearum*. In: National Institute of Agricultural Sciences (Ed.), MAFF Microorganism Genetic Resources Manual No.12. National Institute of Agricultural Sciences, Tsukuba, Japan, pp. 5–8.
Kasman, L.M., Kasman, A., Westwater, C., Dolan, J., Schmidt, M.G., Norris, J.S., 2002. Overcoming the phage replication threshold: a mathematical model with implications for phage therapy. J. Virol. 76, 5557–5564.
Katoh, K., Toh, H., 2008. Recent developments in the MAFFT multiple sequence alignment program. Brief. Bioinform. 9, 286–298.
Kropinski, A.M.B., Bose, R.J., Warren, R.A.J., 1973. 5-(4-Aminobutylaminomethyl)uracil, an unusual pyrimidine from the deoxyribonucleic acid of bacteriophage phiW-14. Biochemistry 12, 151–157.
Kurtz, S., Phillippy, A., Delcher, A.L., Smoot, M., Shumway, M., Antonescu, C., Salzberg, S.L., 2004. Versatile and open software for comparing large genomes. Genome Biol. 5, R12.
Laemmli, U.K., 1970. Cleavage of structural proteins during the assembly of the head of bacteriophage T4. Nature 227, 680–685.
Lavigne, R., Darius, P., Summer, E.J., Seto, D., Mahadevan, P., Nilsson, A.S., Ackermann, H.W., Kropinski, A.M., 2009. Classification of *Myoviridae* bacteriophages using protein sequence similarity. BMC Microbiol. 9, 224.
Lowe, T.M., Eddy, S.R., 1997. tRNAscan-SE: a program for improved detection of transfer RNA genes in genomic sequence. Nucleic Acids Res. 25, 955–964.
Petrov, V., Ratnayaka, S., Nolan, J.M., Miller, E.S., Karam, J.D., 2010. Genomes of the T4-related bacteriophages as windows on microbial genome evolution. Virol. J. 7, 292.

Remenant, B., Coupat-Goutaland, B., Guidot, A., Cellier, G., Wicker, E., Allen, C., Fegan, M., Pruvost, O., Elbaz, M., Calteau, A., Salvignol, G., Mornico, D., Mangenot, S., Barbe, V., Medigue, C., Prior, P., 2010. Genomes of three tomato pathogens within the *Ralstonia solanacearum* species complex reveal significant evolutionary divergence. BMC Genomics 11, 379.

Rohrer, H., Zillig, W., Mailhammer, R., 1975. ADP-ribosylation of DNA-dependent RNA polymerase of *Escherichia coli* by an NAD^+:protein ADP-ribosyltransferase from bacteriophage T4. Eur. J. Biochem. 60, 227–238.

Sambrook, J., Russell, D.W., 2001. Molecular Cloning: A Laboratory Manual. third ed. Cold Spring Harbor Laboratory Press, Cold Spring Harbor, New York N.Y.

Stamatakis, A., 2014. RAxML version 8: a tool for phylogenetic analysis and post-analysis of large phylogenies. Bioinformatics 30, 1312–1313.

Stothard, F., Wishart, D.S., 2005. Circular genome visualization and exploration using CGView. Bioinformatics 21, 537–539.

UniProt Consortium, 2014. UniProt: a hub for information. Nucleic Acids Res. 42, D191–D198.

Wheeler, D.L., Barrett, T., Benson, D.A., Bryant, S.H., Canese, K., Chetvrnin, V., Church, D.M., DiCuccio, M., Edgar, E., Federhen, S., Geer, L.Y., Kapustin, Y., Khovayko, O., Landsman, D., Lipman, D.J., Madden, T.L., Maglott, D.R., Ostell, J., Miller, V., Pruitt, K.D., Schuler, G.D., Sequeira, E., Sherry, S.T., Sirotkin, K., Souvorov, A., Starchenko, G., Tatusov, R.L., Tatusova, T.A., Wagner, L., Yaschenko, E., 2007. Database resources of the National Center for Biotechnology Information. Nucleic Acids Res. 35, D5–D12.

Yabuuchi, E., Kosako, V., Yano, I., Hotta, H., Nishiuchi, Y., 1995. Transfer of two *Burkholderia* and an *Alcaligenes* species to *Ralstonia* gen. nov.: proposal of *Ralstonia picketii* (Ralston, Palleroni and Doudoroff 1973) comb. nov., *Ralstonia solanacearum* (Smith 1896) comb. nov. and *Ralstonia eutropha* (Davis 1969) comb. nov. Microbiol. Immunol. 39, 897–904.

Yamada, T., 2012. Bacteriophages of *Ralstonia solanacearum*: their diversity and utilization as biocontrol agents in agriculture. In: Kurtboke, I. (Ed.), Bacteriophages. InTech-Open Access Publisher, Rijeka, Croatia, pp. 113–139.

Yamada, T., Kawasaki, T., Nagata, S., Fujiwara, A., Usami, S., Fujie, M., 2007. New bacteriophages that infect the phytopathogen *Ralstonia solanacearum*. Microbiology 153, 2630–2639.

Yamada, T., Sato, S., Ishikawa, H., Fujiwara, A., Kawasaki, T., Fujie, M., Ogata, H., 2010. A jumbo phage infecting the phytopathogen *Ralstonia solanacearum* defines a new lineage of the Myovirus family. Virology 398, 135–147.